Structural and electrical characterization of n-InAs/p-GaP heterojunctions prepared by vacuum flash evaporation and liquid phase epitaxy

A. A. M. FARAG[*,a,b], F. S. TERRA[c], A. ASHERY[c], A. M. MANSOUR[c]
[a]*Thin Film laboratory, Physics Department, Faculty of Education, Ain Shams University*
[b]*Physics Department, Faculty of Science and Arts, Aljouf University, KSA*
[c]*Solid State Electronics lab, Physics Department, Physics Division, National Research Center, Dokki, Giza, Egypt*

Thin films of n-InAs were successfully grown on p-GaP single crystalline substrates by using two different techniques (i.e. vacuum flash evaporation technique and liquid phase epitaxy). The elemental composition of the prepared films was confirmed by energy dispersive X-ray spectroscopy. The morphology of the film was characterized by scanning electron microscopy. Electrical characteristics of n-InAs/p-GaP heterojunction, prepared by both vacuum flash evaporation and liquid phase epitaxy were investigated. Current density–voltage and high frequency capacitance–voltage characteristics of the barrier were measured in the temperature range from 300 to 400 K. Analysis of current density–voltage characteristics showed that the forward current might be described by a classical thermal emission theory. The ideality factor of the current density–voltage characteristics was found to be dependent of temperature. The temperature dependence of the barrier height was discussed for both heterojunctions. Analysis of the capacitance–voltage characteristics under high frequency indicates abrupt heterojunction formation for the prepared n-InAs/p-GaP. The comparative studies of the prepared heterojunctions, prepared were also performed. The electrical properties were studied in the frequency range of 10^2–10^6 Hz. The dielectric constant and dielectric loss were analyzed as a function of frequency.

(Received May 15, 2015; accepted February 10, 2017)

Keywords: Thin films, Liquid phase epitaxy, Vacuum flash evaporation, Electrical properties, Dielectric properties

1. Introduction

Application possibilities of semiconducting III-V compounds become much wider with the appearance of solid solutions and heterostructures on their basis [1]. However, great interest to these materials arose with the development of semiconductor lasers based on heterostrutures and of multilayered superlattices [1, 2]. Also, creating of quantum-dimensional devices based on these compounds has become very promising [2].

Indium arsenide, InAs, or indium mono-arsenide, is a semiconductor material, a semiconductor composed of indium and arsenic [3-5]. It has the appearance of grey cubic crystals with a melting point 942 °C. InAs is well known for its high electron mobility and narrow energy bandgap. It is widely used as terahertz radiation source as it is a strong photo-dember emitter [3-5].

Most of the heterostructures were obtained by liquid phase epitaxy (LPE) [6,7], vapor phase epitaxy (VPE) [8], molecular beam epitaxy (MBE)[9] and metal organic chemical vapor deposition (MOCVD)[10]. Advantages and disadvantages of each of the above listed techniques as per details mentioned elsewhere [11]. In this paper, the preparation of n-InAs/p-GaP heterostructure employing both Flash evaporation (FE) technique and liquid phase epitaxy LPE is considered. Moreover, the structural and electrical properties of the two prepared heterojunctions are compared. The current–voltage and capacitance–voltage characteristics in dark at different temperatures are also measured and discussed.

2. Experimental procedure

2.1. Fabrication of n-InAs / p-GaP heterojunction

Single crystal wafer of p-type GaP with (100) orientation and resistivity of~ 5–10 Ω.cm was used as substrate. The substrate was chemically cleaned using the RCA cleaning procedure (i.e. boiling in NH_4 +H_2O_2 +6H_2O for 10 min followed by a 10min boil in HCl +H_2O_2 +6H_2O). Thin films of InAs were prepared on GaP by flash evaporation technique and liquid phase epitaxy. The flash evaporation technique was performed under 10^{-4} Pa onto pre-cleaned GaP substrates held at a temperature of 300K using a high vacuum coating unit (Edwards E 306 A, England). A rapid flash evaporation of InAs was obtained by continuously dropping fine particles of the material onto a hot boat surface, so that numerous discrete evaporation occurs. A sketch of the home-made flash evaporation attachment is shown in Fig. 1(a). The loaded boat temperature was kept constant at the melting point of InAs and the deposition rate was controlled at a value of ~2 nm s^{-1} by the vibration of the home-made flash evaporation attachment. The detailed information about

flash evaporation attachment was described elsewhere by Farag et al.[12].

The technique of LPE was described in detail elsewhere by Farag et al. [13, 14]. The loaded boat was heated up to ~ 600 K and kept at this temperature for 30 min to homogenize the solution and then cooled down to 300 K with a cooling rate of 10 K/min. The growth process was terminated by removing the ready substrate with its upper layer from the solution cell. The schematic diagram of liquid phase epitaxy was shown in Fig. 1 (b).

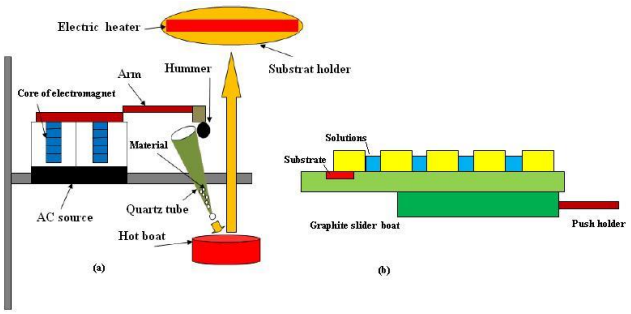

Fig. 1. Sketch of (a) Home-made flash evaporation attachment (b) LPE holder

2.2. Characterization techniques

The film morphology was investigated by scanning electron microscopy (SEM) using model JEOL JXA-8400 A. Chemical composition of the obtained InAs thin films was checked by energy depressive X-ray spectrometry technique (EDX). EDX investigation was carried out by JEOL JXA-8400 A with a link exl EDX detector. The data was corrected using ZAF correction program. Various factors apply which limit the accuracy obtainable in the final result and instrumental instabilities were less than ± 1%, and uncertainty in standard compositions may be similarly small.

X-ray diffraction measurements have been taken by using analytical X'Pert PRO MRD diffractometer system having CuK_{α}, as a radiation source of wavelength $\lambda = 1.540598$ Å with $2\theta = 30°–90°$ at the scan speed 0.5 K/min for the determination of n-InAs/p-GaP heterojunction. The analysis was performed by using Powder Software.

Gold electrode was first evaporated on InAs through suitable mask to form a front ohmic electrode and other gold layer was evaporated on GaP as back electrode to form Au/InAs/GaP/Au heterojunction. The ohimicity of the contacts was checked from the current-voltage characteristics for the contact for both InAs and GaP. The linearity for the specific contacts in each case revealed ohmic behavior with lower electrical resistance. Moreover, the type of polarity of n-type InAs was checked by hot point probe test.

In order to measure the electrical properties of the heterojunction, electrical contacts were equipped with copper wires mechanically applied to the two metal electrodes using thermosetting silver paint. The dark *J–V* characteristics were performed at different temperatures by a high impedance programmable Keithley 617 source meter. The dark *C-V* measurements were performed at different temperatures in the range 300-400 K by maintaining a constant fixed frequency at 1MHz, using a computerized capacitance–voltage system consisting of the 410 *C–V* meter via model 4108 *C–V* interface. The temperature was measured directly by means of chromel–alumel thermocouple connected to hand-held digital thermometer.

3. Results and discussion

3.1. Morphology characterization

SEM micrographs of n-InAs/p-GaP prepared by FE and LPE are shown in Fig. 2 (a) and (b). Two different morphologies of the films are obtained depending on the method of preparation. For the flash evaporated film, the surface is characterized by lower crystalline, lower dense, free of cracks, non-uniform morphology and agglomeration of the film on the surface. This morphology is optimized by using a rotating holder to control the distribution of the InAs film on GaP substrate. Due to comparably high solute concentrations relatively high growth rates can be applied through the LPE growth. The surface morphology of the liquid phase epitaxial InAs on GaP single crystalline substrates is shown in Fig. 2. A well crystalline grain with different sizes and agglomeration grow this observed.

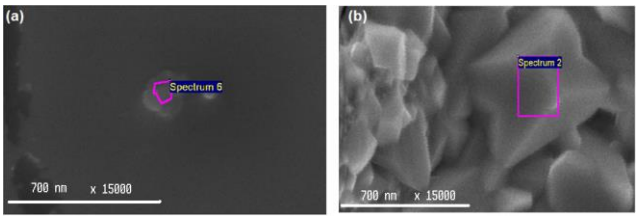

Fig. 2. SEM micrograph of n-InAs/p-GaAs prepared by (a) FE and (b)LPE

3.2. Composition characterization

The EDX spectral analysis for the n-InAs/p-GaP prepared by vacuum flash evaporation technique and liquid phase epitaxy are shown in Fig. 3 (a) and (b), respectively. Fully quantitative analysis results are obtained from the spectrum by processing the data through a correction program. The obtained percentages of the constituent elements in all investigated films indicate that samples prepared by the two methods are nearly stoichiometric with considering an experimental error of about ±1%, tabulated in Table 1. The obtained results give support for the quality of the prepared InAs films by flash evaporation and liquid phase epitaxy techniques.

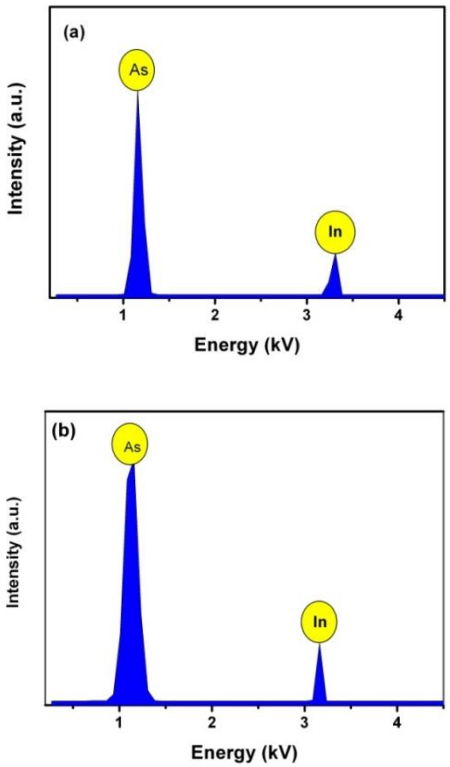

Fig. 3. EDX spectrum of InAs film prepared by (a) FE and (b) LPE

Table 1. EDX results of InAs prepared by FE and LPE techniques. The obtained results with considering of experimental error of ±1%

	FE		*LPE*	
	Weight %	Atomic%	Weight %	Atomic%
In(L)	60.5 ± 0.6	49.9 ± 0.5	60.5 ± 0.6	49.7 ± 0.5
As(K)	39.5 ± 0.4	50.1 ± 0.5	39.5 ± 0.6	50.3 ± 0.5
Total	100	100	100	100

3.3. Crystal characterization

X-ray diffraction patterns, XRD of the n-InAs/p-GaP heterojunction prepared by FE and LPE are shown in Fig. 4(a) and (b). The patterns recorded at an incident angle $2\theta=5^0$ and then does not show any diffraction peaks for the GaP substrate as given in the figures. The diffraction peaks present in the figures are consistent with the standard JCPDS card No. 73-1985 for cubic system of InAs. The maximum intensity in the experimental patterns indicated by (220) and (422) planes corresponding to the identified intensity lines for the standard card gives support for the stability of prepared InAs film.

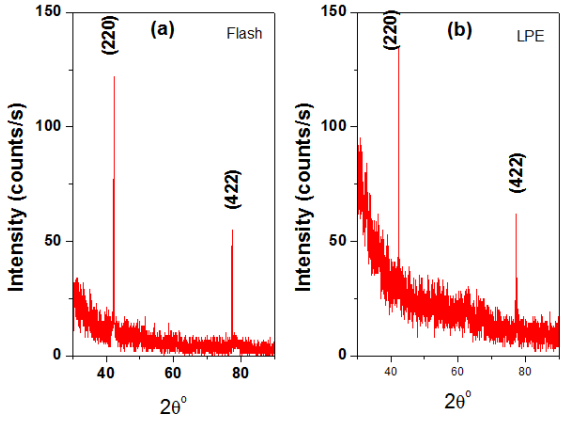

Fig. 4. XRD of n-InAs/p-GaAs prepared by (a) FE and (b) LPE

3.4. Forward J–V characteristics

The forward *J–V* characteristics of n-InAs/p-GaP heterojunctions prepared by FE and LPE are studied in the temperature range 300-400 K. An exponential dependence of forward current on applied voltage is observed in Figs. 5(a) and (b). The *J–V* data were analyzed by using the thermionic emission theory [15]:

$$J = J_s \exp\left(\frac{qV}{nkT}\right)\left(1-\exp\frac{-qV}{kT}\right), \qquad (1)$$

where n is the ideality factor and J_s is the saturation current density which can be identified as follows:

$$J_s = A^* T^2 \exp\left(\frac{-q\Phi_b}{kT}\right) \qquad (2)$$

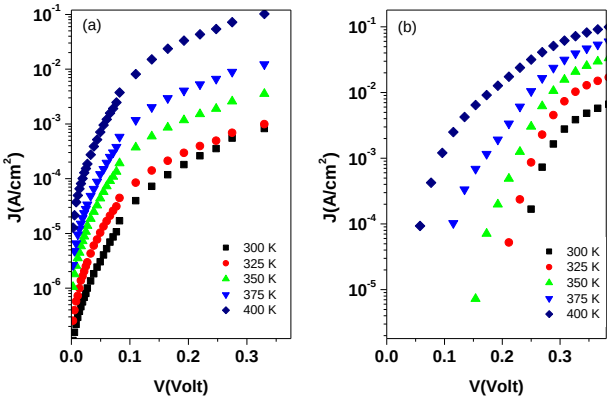

Fig. 5. J-V characteristics of n-InAs/p-GaP heterojunctions prepared by (a) FE and (b) LPE

Using Eq. (1), the values of the ideality factor, n of the junction at different temperatures in the range 300-400 K were calculated from the slope of the linear region of the semi-log forward bias curves. Using Eq. (2), the zero-bias barrier height, Φ_b is determined from the extrapolated

experimental saturation current, J_s. The ideality factor and the zero-bias barrier height at different temperatures are plotted versus temperature, shown in Fig. 6, for the flash evaporated and epitaxially grown n-InAs/p-GaP heterojunctions. From these figures, it is observed that the ideality factor decreases with increasing of temperature but the zero-bias barrier height, Fig. 7 ,increases with increasing temperature. For an ideal junction, the zero-bias barrier height should decrease as temperature is increased, in accordance with the band gap variation with temperature [16-19]. Here, the zero-bias barrier height shows an inverse behavior to the ideality factor variation.

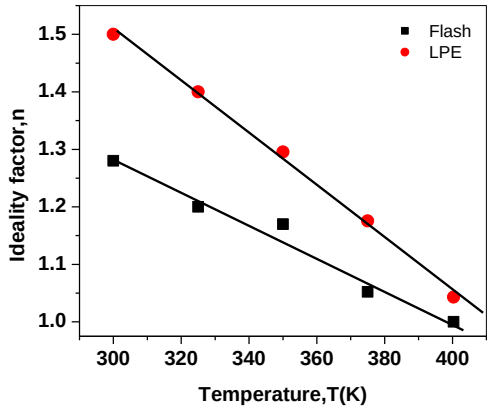

Fig. 6. Temperature dependence of ideality factor for n-InAs/p-GaP heterojunctions prepared by FE and LPE

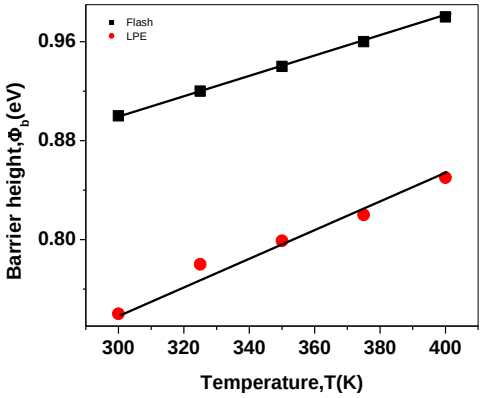

Fig. 7. Temperature dependence of barrier height for n-InAs/p-GaP heterojunctions prepared by FE and LPE

To assess the quality of the grown n-InAs film on p-GaP, several models of conduction mechanisms have been applied to the observed temperature dependent *J–V* data of n-InAs/p-GaP heterojunction. According to Werner–Gütler model [19], the barrier height has a Gaussian distribution with a mean barrier height. The increase in barrier height with increasing temperature has been explained by the lateral distribution of the barrier height [19].

In order to explain the observed variation of ideality factor with temperature in the present case, Werner–Gütler's potential fluctuation model [20] has been considered. According to Tung's model [21, 22], the ideality factor of an inhomogeneous barrier with a distribution of low Schottky barrier heights may increase when the measurement temperature is lowered. As per Sullivan et al. [23] and Tung's model of lateral in homogeneities [21, 22], the Schottky barrier consists of laterally inhomogeneous patches of different barrier heights. The patches with lower barrier height have larger ideality factors and vice versa. Using Tung's theoretical approach, Schmitsdroff et al. [24] found a correlation between the zero-bias barrier height and the ideality factors. The extrapolation of the linear fit to the data gives a homogeneous barrier height an ideality factor of about 1.0. In the present case, the homogeneous barrier height obtained from the linear fit of the zero-bias barrier height versus ideality factor are 0.87 eV and 0.99, respectively for flashy and epitaxilally grown heterojunctions and shown in Fig. 8. According to Schmitsdroff et al. [24], the larger the discrepancy between the homogeneous barrier height and the effective barrier height, the poorer the quality of the grown epilayer. Fig. 9 gives support for the high quality of the flashy or epitaxially grown junctions.

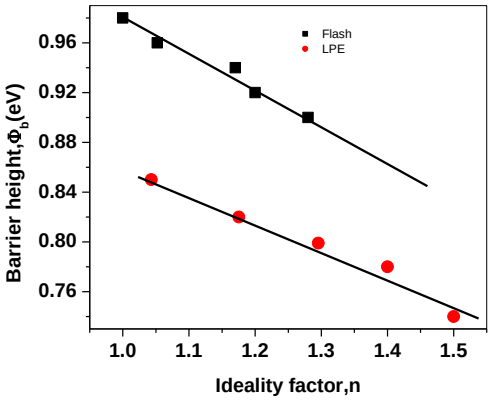

Fig. 8. Barrier height vs. ideality factor of n-InAs/p-GaP heterojunctions prepared by FE and LPE

Fig. 9 presents dependence of J_S/T^2 on $1/T$ for the studied heterojunctions in the temperature range 300-400 K. It is seen that this dependence is exponential, which indicates that thermal emission is responsible for transporting charge carriers through the n-InAs/p-GaP heterojunctions. According to thermionic emission theory, the slope and intercept of this curve give the barrier height Φ_b at 0 K, and Richardson constant. The obtained Φ_b and the effective Richardson constant are found to be 0.45 eV and 1.1 eV and 8.08 A cm^{-2} K^{-2} and 10.45 A cm^{-2} K^{-2}, respectively for the flashy evaporated and epitaxially grown n-InAs/p-GaP heterojunctions. The obtained A^* values for the two heterojunctions are in agreement with those published value, 8.16 A cm^{-2} K^{-2} for GaP [25]. Moreover, it has been reported in the literature that the Richardson constant varies from 3 to 100 A K^{-2} cm^{-2} [25].

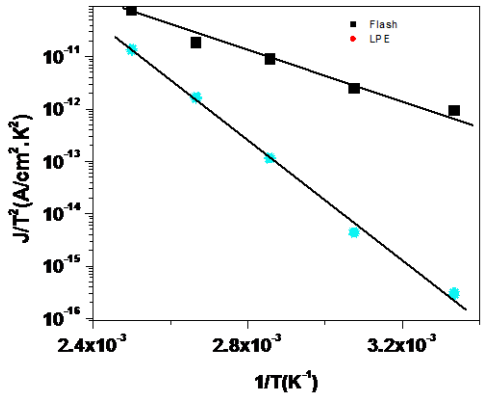

Fig. 9. J/T^2 vs. 1/T of n-InAs/p-GaP heterojunctions Prepared by FE and LPE

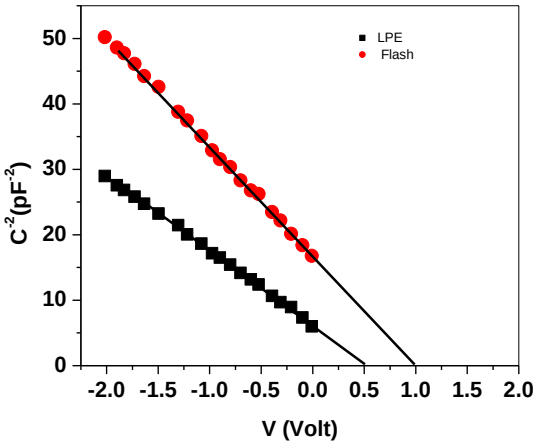

Fig. 10. Plot of C^{-2} vs. V for n-InAs/p-GaP heterojunctions prepared by FE and LPE

3.5. Capacitance - voltage characteristics

The $1/C^2$–V characteristics of n-InAs/p-GaP heterojunctions at room temperature (300 K) for the two prepared heterojunctions are shown in Fig. 10. The obtained good linearity fit for the two cases can reasonably be interpreted by assuming an abrupt heterojunction [26]. This can be due to the assumption of the acceptor concentration of the p-type GaP substrate is small in comparison with those for the donor concentration of the InAs layer. Then, the space charge region of the heterojunction lies mainly on the GaP side and the junction is considered to be abrupt or similar to one sided junction [27,28]. Therefore, the C-V characteristics were analyzed using the equation for the capacitance of a Schottky contact (same as for a one-sided abrupt junction). The relation between the junction capacitance, *C*, and the reverse applied potential for an abrupt junction can be given by the following equation [29]:

$$C^{-2} = -\frac{2(V_{bi} - V - kT/e)}{e\varepsilon N_a A^2}, \qquad (3)$$

Where V_{bi} is the built-in potential, N_a is the free carrier concentration, A is the effective area and ε is the dielectric constant. The acceptor carrier concentration and the built-in potential were easily estimated. The values of V_{bi} and N_a obtained by the capacitance-voltage measurements are calculated and listed in Table 2. The discrepancy between the built-in potential obtained from *C-V* measurement and barrier height obtained from *J-V* measurement could be explained by the existence of excess capacitance at the structure due to the interfacial layer or trap states in the semiconductor and the existence of the barrier inhomogeneity offers another explanation [30].

Table 2. The obtained parameters from C-V measurements for n-InAs/p-GaP heterojunctions

Parameter	*FE*	*LPE*
V_{bi}	1.0	0.5
N_a	5×10^{13} m^{-3}	2×10^{13} m^{-3}

3.6. Dielectric constants measurements

The frequency dependence of both dielectric constant and dielectric loss for InAs/p-GaP heterojunctions prepared by flash evaporation and LPE are shown in Fig. 11(a) and (b). The values of dielectric constant are found to decrease by increasing frequency at lower frequency followed by a leveling off at higher frequency (Fig. 11 a). Variation of dielectric loss as a function of frequency for the two prepared heterojunctions is depicted in Fig. 11(b). Obviously, the magnitude of dielectric loss is found to be decrease with increasing frequency. Moreover, in Fig. 11 (a), one can see that the dielectric constant values are higher at low frequency (less than 10^4 Hz) and followed by a sharp decrease as the frequencies are increased. Generally, the behavior at low frequency can be explained by the interfacial polarization which decreases with increasing frequency and can be attributed to differences in the conductivity of the material. At high frequency the permittivity has contributions as from atomic and ionic polarizations. From Fig. 11(b), the high values of dielectric loss for the two heterojunctions in the low frequency region can be attributed to the dielectric relaxation arising from the interfacial polarization [30].

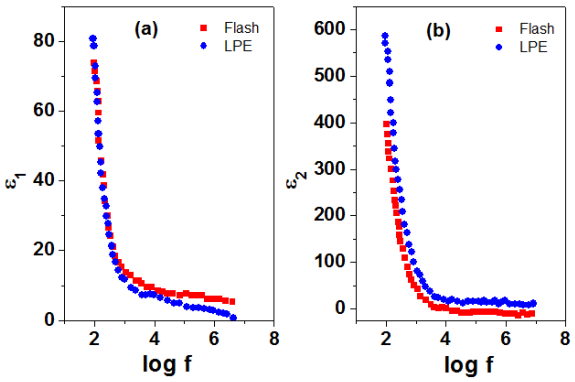

Fig. 11. (a) Variation of dielectric constant and (b) dielectric loss with frequency for n-InAs/p-GaP heterojunctions prepared by FE and LPE

4. Conclusions

The current density–voltage characteristics of InAs/p-GaP heterojunctions, prepared by FE and LPE in the temperature range of 300-400 K, show high rectification characteristics. The zero-bias barrier height increases and the ideality factor decreases with increasing temperature. The small discrepancies between the experimental and theoretical values of the barrier height and ideality factor could be due to deviations in the barrier height distribution from the Gaussian model assumed by Werner–Gütler. According to Tung's approach of lateral inhomogeneities, the homogeneous barrier height and the effective barrier heights are closely matched, which shows a good quality of the InAs film grown on the GaP substrate. The value of the Richardson constant is close to the value used for the determination of the zero-bias barrier height. The quality of the grown n-InAs film on the p-GaP substrate by thermal evaporation and liquid phase epitaxy is good, based on the results of electrical characterization. *C–V* measurements indicate that acceptor-like surface states exist in the epitaxial layer grown of InAs on the GaP substrate and donor-like states in the epitaxial layer grown on the conventional part of the substrate, which affect the *C–V* characteristics. Dielectric properties at lower frequencies are primarily due to interfacial polarization. The dielectric constant and dielectric loss decreased with increase in frequency.

References

[1] S. J. Polly, C. G. Bailey, A. J. Grede, D. V. Forbes, S. M. Hubbard, Journal of Crystal Growth **454**, 64 (2016).

[2] Z. Guo, J. Mu, Y. Lian, Z. Li, J. Alloys Compd. **690**, 160 (2017).

[3] M. S. Al-Ghamdi, A. Sayari, L. Sfaxi, J. Alloys Compd. **685**, 202 (2016).

[4] A. Reklaitis, Optics Commun. **371**, 221 (2016).

[5] T. Woldu, B. Raneesh, B. Krishna Hazra, S. Srinath, P. Saravanan, M. V. Ramana Reddy, N. Kalarikkal, J. Alloys Compd. **691**, 644 (2017).

[6] Yu Zorenko, T. Zorenko, V. Gorbenko, T. Voznyak, P. Popielarski, M. Batentschuk, A. Osvet, Ch. Brabec, V. Kolobanov, D. Spasky, A. Fedorov, Rad. Measur. **90**, 132 (2016).

[7] R. Wutzler, L. Rebohle, S. Prucnal, R. Hübner, S. Facsko, R. Böttger, M. Helm, W. Skorupa, Mater. Sci. Semicond. Proc. **42**, 166 (2016).

[8] K. L. Schulte, J. Simon, A. Roy, R. C. Reedy, D. L. Young, T. F. Kuech, A. J. Ptak, J. Cryst. Growth **434**, 138 (2016).

[9] M. Debiossac, P. Atkinson, A. Zugarramurdi, M. Eddrief, F. Finocchi, V. H. Etgens, A. Momeni, H. Khemliche, A. G. Borisov, P. Roncin, Appl. Surf. Sci. **391**, 53 (2017).

[10] B. Hertog, O. Ledyaev, D. Volovik, R. Miller, A. Osinsky, S. Bakhshi, W. V. Schoenfeld, Sens. Actuat. A **249**, 263 (2016).

[11] Y. J. Jin, X. H. Tang, C. Ke, D. H. Zhang, Thin Solid Films **616**, 624 (2016).

[12] A. A. M. Farag, F. S. Terra, G. M. M. Fahim, A. Ashery, Mahmoud Nasr, M. M. EL Okr, Optoelectron. Adv. Mat. **7**(5-6), 381 (2013).

[13] A. A. M. Farag, G. M. Mahmoud, F. S. Terra, M. M. El Nahass, Phys. Low Dim. Struct. **5/6**, 1 (2004).

[14] A. A. M. Farag, F. S. Terra, G. M. Mahmoud, M. Mounir Saad El-Din, Phys. Low Dim. Struct.**7/8**, 45 (2004).

[15] E. H. Rhoderick, Metal–Semiconductor Contacts (Clarendon Press, Oxford) (1978).

[16] S. Hardikar, M. K. Hudait, P. Modak, S. Krupanidhi, N. Padha, Appl. Phys. A **68**, 49 (1999).

[17] S. M. Sze, Physics of Semiconductor Devices 2nd ed.(USA, NewYork: Wiley) (1981).

[18] R. Hackam, P. Harrop, IEEE Trans Electron. Dev. ED **19**, 1231 (1972).

[19] M. B. Panish, H. C. Casey, J. Appl. Phys. **40**, 1663 (1969).

[20] J. H. Werner, H. H. Güttler, J. Appl. Phys. **69**, 1522 (1991).

[21] R. T. Tung, Phys. Rev. B **45**1, 3509 (1992).

[22] R. T. Tung, J. P. Sullivan, F. Schrey, Mat. Sci. Eng. B **14**, 266 (1992).

[23] J. P. Sullivan, R. T. Tung, M. R. Pinto, W. R. Graham, J. Appl. Phys.**70**, 7403 (1991).

[24] R. F. Schmitsdorf, T. U. Kampen, W. Monch, J. Vac. Sci. Technol. B**15**, 1221 (1997).

[25] A. K. Srivastava, B. M. Arora, S. Guha, Solid-State Electron. **24**, 185 (1981).

[26] M. K. Hudait, P. Modak, S. Hardikar, S.B. Krupanidhi, J. Appl. Phys. **83**, 4454 (1998).

[26] A. A. M. Farag, H. S. Solimanan, A. A. Atta, Synthetic Metals **161**, 2759 (2012).

[27] C. Nguyen Van, K. Potje-Kamloth, Thin Solid Films **392**, 113 (2001).

[28] A. A. M. Farag, A. Ashery, F. S. Terra, Microelectronics Journal **39**, 253 (2008).

[29] A. A. M. Farag, F. S. Terra, G. M. Mahmoud, A. M. Mansour, Alloys Compd. **481**, 427 (2009).

[30] J. Jobish, N. Charoen, P. Praveen, J. Non-Crystalline Solids **358**, 1113 (2012).

*Corresponding author: alaafaragg@gmail.com
aamfaraj@ju.edu.sa